2018 Annual American Control Conference (ACC)
June 27–29, 2018. Wisconsin Center, Milwaukee, USA

Vibrational Control in Flapping-Wing Micro-Air-Vehicles

Haithem Taha[1], Mohammadali Kiani[2] and Joel Navarro[3]

***Abstract*— Flapping-Wing Micro-Air-Vehicles (FWMAVs) are bio-inspired air vehicles that mimic insect and bird flight. The dynamic behavior of these systems is typically described by a multi-body, multi-time-scale, nonlinear, time-varying dynamical system. Interestingly, this rich dynamics lead to unconventional stabilization mechanisms whose study essentially necessitates a mathematically rigorous analysis. In this paper, we use higher-order averaging, which is based on chronological calculus, to show that insects and their man-made counterparts (FWMAVs) exploit *vibrational control* to stabilize their body pitching angle. Such an unconventional stabilization cannot be captured by direct averaging. We also experimentally demonstrate such a phenomenon by constructing an experimental setup that allows for two degrees of freedom for the body; forward motion and pitching motion. We measure the response of the body pitching angle using a digital camera and an image processing algorithm at different flapping frequencies. It is found that there is a flapping frequency threshold beyond which the body pitching response is *naturally* (without feedback) stabilized, which conforms with the vibrational control concept. Moreover, we also construct a replica of the experimental setup with the FWMAV being replaced by a propeller revolving at constant speed, which results in a constant aerodynamic force, leaving no room for vibrational control. The response of the propeller-setup is unstable at all frequencies, which also corroborates the fact that the observed stabilization of the FWMAV-setup at high frequencies is a vibrational stabilization phenomenon.**

I. Introduction

Vibrational control is an open loop stabilization technique of an unstable equilibrium via the application of a sufficiently high-amplitude, high-frequency periodic forcing. For example, the unstable equilibrium of the inverted pendulum gains asymptotic stability when the pivot is oscillating vertically at a sufficiently high frequency. Crude averaging of the simple equations governing the dynamics of the Kapitza pendulum [1], [2] (inverted pendulum whose pivot is subject to a vertical oscillation) showed no stabilization due to the pivot vibration. However, appropriate averaging techniques; whether it is higher-order averaging [3], [4] based on chronological calculus [5]; higher-order averaging [6], [7] based on Lie transform [8]; direct averaging exploiting the nonlinear variation of constants formula [9], [10]; clearly show a vibrationally-induced stabilizing stiffness.

Flapping-wing micro-air-vehicles (FWMAVs) represent a rich dynamical system with unconventional dynamical behavior that caught the attention of biologists and engineers over the last two decades. The multi-body dynamics of FWMAVs is typically described by nonlinear, time-periodic (NLTP) models. Moreover, the fast oscillatory wing motion and its associated inertial and aerodynamic loads interact with the relatively slower body motion resulting in a multi-time-scale dynamical system. These features lead to interesting unconventional balance and stability characteristics, which invoke a mathematically rigorous analysis.

While many research reports (e.g., [11]–[22]) concluded an unstable flight dynamics for hovering insects and FWMAVs; mainly due to lack of pitch stiffness, the recent efforts by Taha et al. [23]–[26] showed an induced vibrational stabilization mechanism in the form of pitch stiffness on the flight dynamics of these bio-inspired robots. In this paper, we theoretically and experimentally demonstrate the vibrational control phenomenon in the flight of FWMAVs. We use higher-order averaging to show the vibrationally-induced pitch stiffness. Moreover, we experimentally demonstrate such a phenomenon on a flapping apparatus that allows two degrees-of-freedom (DOF) for the body of a FWMAV .

II. Flight Dynamics of FWMAVs

A. Flight Dynamic Modeling

Figure 1 shows a schematic diagram for a FWMAV in the longitudinal plane $x-z$ with three DOF: translations along the x and z axes with velocity components u and w, respectively, and a rotation about the y axis (into the page) represented by an angle θ and an angular velocity q. The generalized forces X and Z are the aerodynamic forces in the x- and z-directions, respectively, and M is the aerodynamic pitching moment about the y-axis. Ignoring the

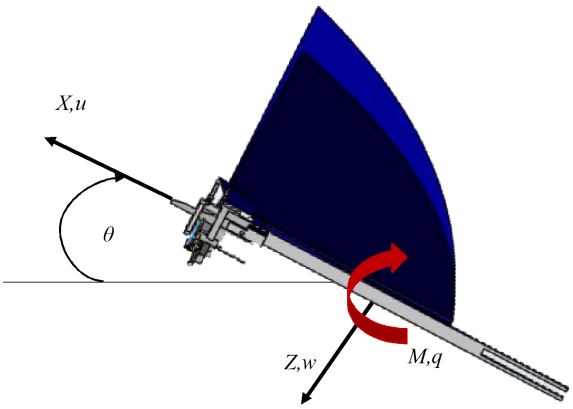

Fig. 1. Schematic diagram of a FWMAV in the longitudinal plane $x-z$.

wing structural and inertial effects, the longitudinal equations

[1]Assistant Professor, Mechanical and Aerospace Engineering, University of California, Irvine, CA hetaha@uci.edu
[2]Master Student, Mechanical and Aerospace Engineering, University of California, Irvine, CA mkiani@uci.edu
[3]Undergraduate Student, Ecole Nationale Superieure de Mecanique et d'Aerotechnique, Chasseneuil-du-Poitou, France joel.navarro@sfr.fr. This work is performed at UCI.

of motion are exactly the same as conventional aircraft [27]

$$\begin{pmatrix} \dot{u} \\ \dot{w} \\ \dot{q} \\ \dot{\theta} \end{pmatrix} = \begin{pmatrix} -qw - g\sin\theta \\ qu + g\cos\theta \\ 0 \\ q \end{pmatrix} + \begin{pmatrix} X/m \\ Z/m \\ M/I_y \\ 0 \end{pmatrix}, \quad (1)$$

where g is the gravitational acceleration, m is the body mass, and I_y is the body pitching inertia. However, unlike conventional aircraft, the aerodynamic loads X, Z, and M are essentially time-varying. That is, the system (1) can be written in the abstract form

$$\dot{\boldsymbol{x}}(t) = \boldsymbol{F}(\boldsymbol{x}(t), \tau) = \boldsymbol{f}(\boldsymbol{x}(t)) + \boldsymbol{g}_a(\boldsymbol{x}(t), \tau), \quad (2)$$

where the aerodynamic vector field $\boldsymbol{g}_a$ is time varying.

It is quite important to note that two symbols t and τ are used in Eq. (2) to denote the independent time variable; to distinguish between the slow time scale t associated with the body motion and the fast time scale associated with the concomitant flapping motion and aerodynamic loads. The ratio between these two time scales is deceptively large; for the slowest flapping insect (the hawkmoth), the ratio between the flapping frequency and the flight dynamics natural frequency is around 30 [15], [28], which naturally invokes averaging. That is, the aerodynamic loads oscillates with a too high frequency to affect the body. In other words, the body only responds to the mean values of the time-periodic aerodynamic loads. This assumption is found in most of flapping flight dynamics and control efforts [11], [12], [14]–[16], [29]–[40]. Adopting this averaging assumption, the averaged dynamics of the system (2) is written as

$$\dot{\bar{\boldsymbol{x}}} = \bar{\boldsymbol{F}}(\boldsymbol{x}(t)) = \boldsymbol{f}(\bar{\boldsymbol{x}}) + \bar{\boldsymbol{g}}_a(\bar{\boldsymbol{x}}), \quad (3)$$

where over bar indicates an averaged quantity; e.g., $\bar{\boldsymbol{g}}_a(\boldsymbol{x}) = \frac{1}{T}\int_0^T \boldsymbol{g}_a(\boldsymbol{x}, \tau) d\tau$, with T being the flapping period.

Following our previously derived aerodynamic model [28], [41], which is based on Refs. [42]–[44], the aerodynamic loads can be expressed linearly in the state variables $\boldsymbol{x}$, near the hovering position as

$$\boldsymbol{g}_a(\boldsymbol{x}(t), \tau) = \boldsymbol{g}_0(\tau) + [\boldsymbol{G}(\tau)]\, \boldsymbol{x}(t), \quad (4)$$

where $\boldsymbol{g}_0$ represents the aerodynamic loads due to flapping, ignoring the effect of body motion (i.e., ignoring aerodynamic-dynamic interactions), and the matrix $\boldsymbol{G}$ represents the aerodynamic derivatives (i.e., stability derivatives) with respect to the state variables. Expressions of the various terms in $\boldsymbol{g}_0$ and $\boldsymbol{G}$ are given in terms of the flapping kinematics in our previous efforts [23], [28], [41].

B. Stability Analysis Using Direct Averaging

Direct averaging greatly simplifies the problem as it converts the time-periodic system (2) into a time-invariant system (3). Consequently, a periodic orbit representing an equilibrium solution of (2) reduces to a fixed point of the averaged dynamics (3). Clearly, the stability analysis of a fixed point of a time-invariant system is quite simpler than that of a periodic solution for a time-periodic system. Luckily, the averaging theorem [9], [45] guarantees exponential stability of a periodic solution of (2) if the corresponding fixed point of (3) is exponentially stable.

To focus on the open-loop stability, we will exclude the non-trivial balance problem in this paper; that is, we assume that the FWMAV is balanced at hover; i.e., equivalently, the averaged dynamics has a fixed point at the origin

$$\boldsymbol{f}(\boldsymbol{0}) + \bar{\boldsymbol{g}}_0 = \boldsymbol{0} \Longleftrightarrow \bar{Z}_0 = -mg.$$

Then, linearizing the averaged dynamics (3) about this fixed point at the origin yields

$$\dot{\bar{\boldsymbol{x}}}(t) = \left[D\boldsymbol{f}(\boldsymbol{0}) + \bar{\boldsymbol{G}}\right] \bar{\boldsymbol{x}}(t), \quad (5)$$

where $D\boldsymbol{f}(\boldsymbol{0})$ is the jacobian of the vector field $\boldsymbol{f}$ at the origin and $\bar{\boldsymbol{G}}$ represents the cycle-averaged stability derivatives. Evaluating the matrix of the linearized system (5) for the hawkmoth insect, whose morphological parameters are adopted from Refs. [15], [23], [46], one obtains

$$\left[D\boldsymbol{f}(\boldsymbol{0}) + \bar{\boldsymbol{G}}\right] = \begin{bmatrix} -3.59 & 0 & 0 & -9.81 \\ 0 & -3.30 & 0 & 0 \\ 39.95 & 0 & -7.92 & 0 \\ 0 & 0 & 1 & 0 \end{bmatrix}$$

whose eigenvalues are written as

$$0.19 \pm 5.74i,\ -11.89,\ -3.30.$$

These eigenvalues indicate an unstable system due to the pair in the right half plane, which are mainly associated with pitching motion as can be easily shown by checking the corresponding eigenvectors. This result is well known and has been concluded in several efforts [11], [12], [14]–[16], [21], [22], [28], [47]–[49].

III. Higher-Order Averaging and Vibrational Control

As in the case with the Kapitza pendulum, the crude averaging analysis, explained above, does not capture vibrational stabilization. One remedy is to use the variation of constants formula (coordinate transformation) to write the system (2) in the standard form of first-order averaging. However, this process is not analytically tractable here. Alternatively, one can use higher-order averaging to reveal higher-order interactions between the system's two time scales that are typically neglected by direct averaging.

Agrachev and Gamkrelidze wrote a seminal paper [5] in the honor of the 70^{th} birth day of the pioneer Russian mathematician Lev Semyonovich Pontryagin which laid down the foundation of a new calculus for time-varying vector fields; the *chronological calculus*. Based on these tools, Sarychev [3] and Vela [4] developed what they called the *complete averaging* of the time-periodic system (2) as an infinite series

$$\dot{\bar{\boldsymbol{x}}} = \epsilon \boldsymbol{\Lambda}_1(\bar{\boldsymbol{x}}) + \epsilon^2 \boldsymbol{\Lambda}_2(\bar{\boldsymbol{x}}) + ..., \quad (6)$$

where ϵ is a small parameter, typically scaled with the reciprocal of the forcing frequency, and

$$\begin{aligned} \boldsymbol{\Lambda}_1(\bar{\boldsymbol{x}}) &= \tfrac{1}{T}\int_0^T \boldsymbol{F}(\boldsymbol{x}, \tau)\, d\tau, \\ \boldsymbol{\Lambda}_2(\bar{\boldsymbol{x}}) &= \tfrac{1}{2T}\int_0^T \left[\int_0^\tau \boldsymbol{F}(\boldsymbol{x}, s)\, ds, \boldsymbol{F}(\boldsymbol{x}, \tau)\right] d\tau. \end{aligned}$$

So, if the flapping frequency is high enough (i.e., ϵ is small enough), one may be able to truncate the series (6) after the first term $\mathbf{\Lambda}_1$ (i.e., crude averaging). However, if the flapping frequency is not high, one should take into account more terms in the series. For more details about this approach, the reader is referred to the Refs. [3], [4], [23].

Taking two terms in the series (6) and linearizing about the origin, one obtains the following system matrix for the hawkmoth linearized hovering dynamics

$$D(\mathbf{\Lambda}_1+\mathbf{\Lambda}_2)(\mathbf{0})=\begin{bmatrix} -3.58 & 0 & 0 & -9.81 \\ 0 & -3.09 & 0 & 0 \\ 29.98 & 0 & -8.13 & -28.45 \\ -2.90 & 0 & 0.96 & 0 \end{bmatrix}$$

whose eigenvalues are written as

$$-0.66 \pm 3.72i,\ -10.40,\ -3.09$$

which indicate a stable system.

This stabilization is not captured by crude averaging. To determine the nature of this *vibrarional stabilizing* mechanism, which is induced by higher-order interactions between the system's two times scales, we compare the two matrices $D(\mathbf{\Lambda}_1)(\mathbf{0})$, $D(\mathbf{\Lambda}_1+\mathbf{\Lambda}_2)(\mathbf{0})$ of the first- and second-order averaged dynamics, respectively. Of particular interest is the element (3,4), which represents pitch stiffness. It is found that the original hovering flight dynamics of insects and FWMAVs lacks any *direct* pitch-stiffness [28]. However, higher-order averaging revealed a vibrationally-induced pitch-stiffness, which is written as

$$\dot{\bar{q}}=\ddot{\bar{\theta}}=-28.45\bar{\theta}.$$

This vibrational control stiffness is quite similar to the Kapitza pendulum case, which can be clearly seen in the interesting video in Ref. [50]. Thanks to the analytical nature of the presented model and analysis tool, we managed to drive an analytical expression of this vibrationally induced stiffness in terms of insect morphological parameters as

$$k_\theta=\frac{g}{2T}\int_0^T\left[M_u(t)t-\int_0^t M_u(\tau)d\tau\right]dt=\frac{mg^2f(\Phi)}{2I_y\bar{\dot{\varphi}}^2}, \tag{7}$$

where M_u is the pitching moment due to disturbance in the body speed, Φ is the flapping amplitude, $\bar{\dot{\varphi}}$ is the average flapping speed, and $f(\Phi)=\frac{\sin 2\Phi}{2\Phi}-\cos 2\Phi$.

IV. Experimental Demonstration

In this section, we experimentally demonstrate the vibrational control phenomenon in FWMAVs. In order to avoid the many problems associated with the free flight of FWMAVs and to have a better focus on verifying the vibrational stabilization phenomenon, we construct an experimental setup that allows for only two DOFs for the body of the FWMAV; forward motion and pitching motion. These two DOFs are particularly selected for demonstration of the vibrational stabilization phenomenon because Eq.(7) implies that k_θ is mainly due to interactions between the pitching and forward motions of the body. Therefore, the proposed experimental setup will represent projection of the full dynamics (1) onto the u_θ sub-system.

Imagine a simple pendulum with its mass replaced by a FWMAV, as shown in Fig. 2. The hovering equilibrium is then achieved when the pendulum's rod becomes horizontal ($\gamma=90^\circ$). This pendulum setup will allow for multiple equilibria at different frequencies; convenient to demonstrate vibrational control, which is evident only at high enough frequencies. One can easily operate at a slower flapping frequency, which results in a different equilibrium *position* γ_e. In addition, measurement of this equilibrium pendulum angle γ_e is easily achieved using a Gravity 360 Degree Hall Angle Sensor and provides a a measure for the generated thrust from the FWMAV as the flapping frequency changes, according to the balance equation

$$F_T=\left(m_{\text{FWMAV}}+\frac{1}{2}m_{\text{rod}}\right)g\sin\gamma_e,$$

where F_T is the cycle-averaged generated thrust force, m_{FWMAV} is the mass of the FWMAV (13 gm), m_{rod} is the mass of the pendulum's rod (1.8 gm), and g is the gravitational acceleration. As the applied voltage is increased, the flapping frequency increases and the FWMAV rises up (i.e., γ_e increases). At each applied voltage, a video is recorded at a rate of 240 frame per second whose time stamp is analyzed to obtain an estimate for the flapping frequency (the average flaps per second).

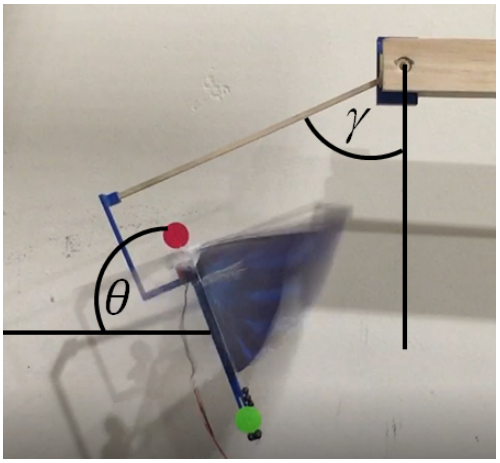

Fig. 2. Two-DOF FWMAV Experimental Setup.

A pin (hinge) connection is introduced between the body of the FWMAV and the pendulum's rod to allow for body pitching θ, as shown in Fig. 2. The response of the pitching angle is measured using a digital camera and an image processing algorithm. As shown in Fig. 2, the nose and tail of the FWMAV are marked with different colors. Then, a simple algorithm is implemented ncy changes, according to the balance equation

$$F_T=\left(m_{\text{FWMAV}}+\frac{1}{2}m_{\text{rod}}\right)g\sin\gamma_e,$$

where F_T is the cycle-averaged generated thrust force, m_{FWMAV} is the mass of the FWMAV (13 gm), m_{rod} is

the mass of the pendulum's rod (1.8 gm), and g is the gravitational acceleration. As the applied voltage is increased, the flapping frequency increases and the FWMAV rises up (i.e., γ_e increases). At each applied voltage, a video is recorded at a rate of 240 frame per second whose time stamp is analyzed to obtain an estimate for the flapping frequency (the average flaps per second).in Visual Studio C++, exploiting the image processing library OpenCV, to detect these circular stickers from video recordings and determine the angle between the line connecting these two marks and the horizontal (i.e. θ) at each time step with a sampling frequency of 50 ms.

Because the line of action of the thrust force is above the body longitudinal axis and consequently hinge point, there is an unbalanced pitching moment which will preclude equilibria. Therefore, we added four split shot size lead of 3g total weight near the tail of the FWMAV, as shown in Fig. 2 (the black dots near tail) to shift the center of gravity of the FWMAV backward along the longitudinal axis. As such, the pitching moment at the hinge point due to the weight will balance that of the thrust force according to the balance equation

$$F_T e_T = mge_g \cos\theta_e,$$

where e_T and e_g are the offsets of the thrust and gravity forces, respectively, from the hinge point, and θ_e is the equilibrium value of the pitching angle. At zero applied voltage (zero thrust force), the FWMAV is standing vertically ($\theta_e = 90°$) at the bottom position ($\gamma_e = 0°$) of the pendulum. As the voltage and consequently the flapping frequency increase, the body moves upward along the circular path of the pendulum (i.e., γ increases) and tilts forward towards the horizontal attitude (i.e., θ decreases), as shown in Fig. 2. It is noteworthy to mention that most insects have their center of gravity behind the hinge location along their longitudinal axis and achieve hovering equilibria at body inclination with respect to the horizontal (i.e., θ_e) around $50°$ [15], [46]; i.e., similar to the current setup.

Having established equilibrium, studying stability comes promptly. To experimentally verify and demonstrate the vibrational control/stabilization phenomenon in FWMAVs, theoretically shown using higher-order averaging in the last section, we apply different voltages to the motor driving the flapping mechanism to attain different equilibrium positions (γ_e and θ_e) at different flapping frequencies, thanks to the pendulum configuration. We then measure the response of the pendulum angle γ and the body pitching angle θ, as explained above, at each operating frequency.

Figure 3 shows the response of the FWMAV system at a flapping frequency of 12Hz. At this low flapping frequency, the FWMAV barely goes up ($\gamma_e \sim 24°$) and the equilibrium pitching angle is quite large ($\theta_e \sim 76°$). The response is found to be unstable as shown in the figure, even without giving a disturbance; the oscillatory wing motion naturally provides a sufficient disturbance.

Figure 4 shows the response of the FWMAV system at a relatively high flapping frequency of 18Hz. At this relatively high flapping frequency, the FWMAV system is almost at the

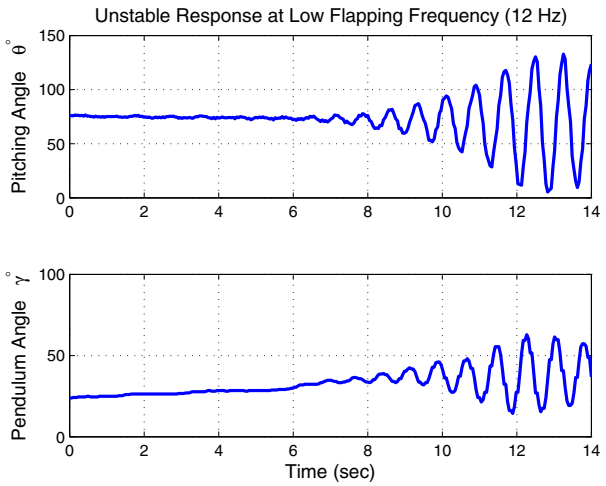

Fig. 3. FWMAV unstable response at relatively low flapping frequency (12Hz).

hovering position ($\gamma_e \sim 85°$) and the equilibrium pitching angle $\theta_e \sim 50°$ is close to the natural values observed in nature for hovering insects [15], [46]. Clearly, the response is stable. Even when a relatively large disturbance ($\Delta\theta \sim 50°$) is applied at $t = 8.6$ sec, the system goes back to its equilibrium periodic orbit (i.e., the hovering periodic orbit). A response similar to that shown in Fig. 4 is observed all possible higher frequencies.

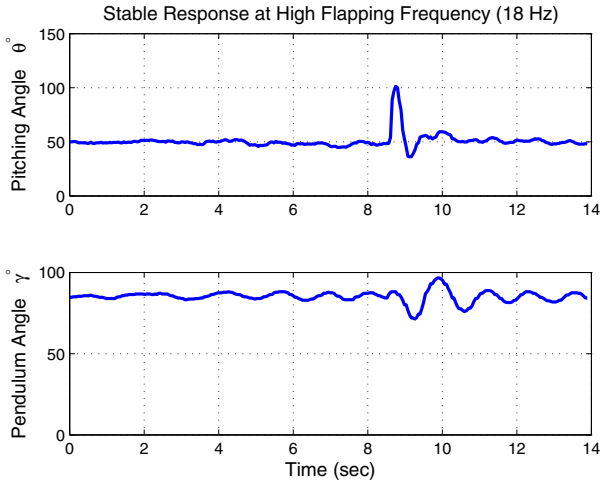

Fig. 4. FWMAV stable response at relatively high flapping frequency (18Hz).

So far, it can be concluded that the response of FWMAVs (particularly the body pitch response) is naturally (without feedback) stabilized beyond a certain threshold of flapping frequency. This fact conforms well with the vibrational control concept [1], [2], [51], [52] and suggests that the observed natural stabilization at high forcing frequencies is a vibrational stabilization phenomenon. However, one might argue that because the intricate dynamics of the system, the frequency not only affects stability, but also bal-

ance/equilibrium; obviously increasing the frequency leads to a different equilibrium, which may or may not have similar stability characteristics to equilibria corresponding to low frequencies. To show that the induced stabilizing mechanism is indeed due to vibrational control that mainly stems from the time-periodic nature of the driving aerodynamic thrust force and not because of operating at a different equilibrium, we construct a replica of the experimental setup with the FWMAV being replaced by a small propeller revolving with a constant speed, as shown in Fig. 5. The main difference is that the FWMAV setup produces a periodic thrust force, and consequently a time-periodic dynamics allowing for vibrational control, while the propeller setup produces a constant thrust force, and consequently a time-invariant dynamics leaving no room for vibrational control.

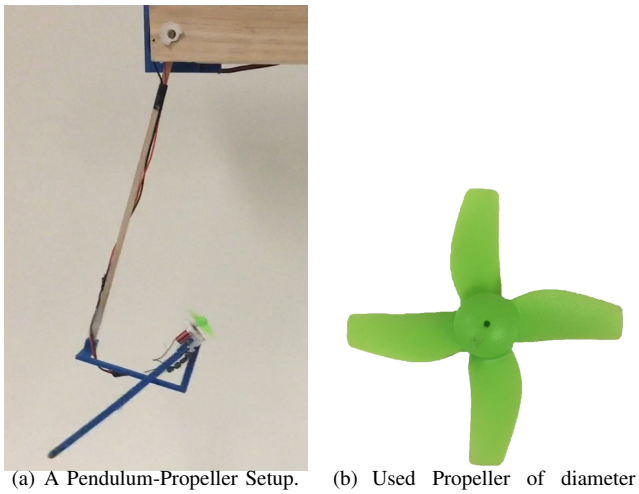

(a) A Pendulum-Propeller Setup. (b) Used Propeller of diameter 3mm.

Fig. 5. A Two-DOF Pendulum-Propeller Setup.

Using split shot size lead, we managed to match the weight and inertia of the propeller system with the FWMAV system. Although the propeller system may experience gyroscopic effects that are different from the flapping system, these gyroscopic actions would not affect the $u - \theta$ dynamics. Rather, they might excite the structural (bending) dynamics of the rod, which is legitimately neglected in this analysis. In fact, the propeller system can be viewed as the crude-average of the flapping system; i.e., the flapping system under the influence of the averaged thrust force after removing the high-frequency varying component. Figure 6 shows the response of the two-DOF propeller-pendulum system at a relatively small propeller speed (i.e., at a small pendulum equilibrium angle $\gamma_e \sim 9°$). Clearly, the response is exponentially unstable. Increasing the applied voltage to attain higher pendulum equilibrium angles (closer to the hovering position) worsens the stability characteristics so much that the system structure becomes prone to breaking.

V. Conclusion

The flight dynamics of insects and their man-made counterparts, flapping-wing micro-air-vehicles (FWMAVs), is studied in the longitudinal plane at hover. The system is a nonlinear, time-periodic with a large separation between

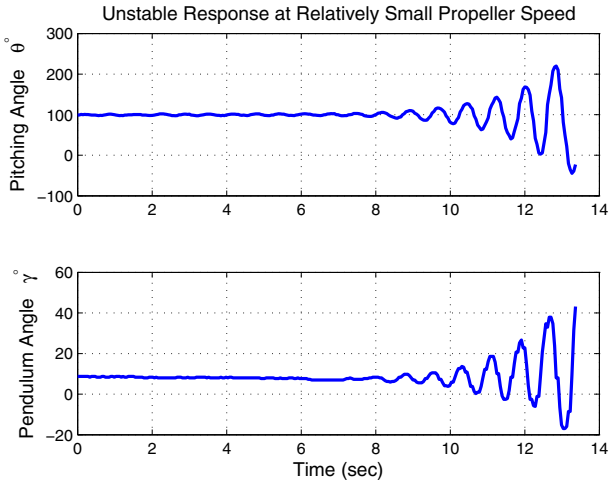

Fig. 6. Unstable Response of the Two-DOF Propeller-Pendulum System.

the systems's two time scales, which invokes averaging. Using direct averaging, it is found that insects/FWMAVs are unstable at hover; mainly due to lack of pitc stiffness. However, using more rigorous mathematical tools (higher-order averaging based on chronological calculus), it is shown that the high-frequency oscillatory aerodynamic forces induce a vibrational control mechanism resulting in a pitch stiffness on the hovering flight dynamics. This unconventional stabilization technique is mainly due to the interaction between the fast wing flapping dynamics and the slow body dynamics, which cannot be captured by direct averaging. An experimental setup that allows for two degrees of freedom for the body (forward motion and pitching motion) is constructed to verify/demonstrate such a phenomenon. Recalling that vibrational control is an *open loop* stabilization technique due to the application of a *sufficiently high frequency periodic forcing*, the stability of the system is studied at different flapping frequencies. It is found that the system is naturally (without feedback) stabilized beyond a certain threshold of the flapping frequency (15Hz in the current setup), which conforms with the vibrational control concept. Moreover, a replica of the system is constructed in which the flapping bird is replaced with a propeller that revolves at a constant speed to check whether the induced stabilization at high frequencies is mainly due to periodicity of the driving force (i.e., a vibrational control) or not. It is found that the propeller system replica is unstable at all applied voltages and becomes even more unstable at larger applied voltages (i.e., when it comes closer to the hovering position). Finally, it is concluded that FWMAVs, indeed, enjoy vibrational stabilization.

VI. Acknowledgment

The first author is thankful to the support of the National Science Foundation grant CMMI-1709746.

References

[1] P. L. Kapitza. Pendulum with a vibrating suspension. *Uspekhi Fiz. Nauk*, 44(1):7–20, 1951.

[2] P. L. Kapitza. Dynamical stability of a pendulum when its point of suspension vibrates. *Collected Papers by PL Kapitza*, 2:714–725, 1965.

[3] A. Sarychev. Stability criteria for time-periodic systems via high-order averaging techniques. In *Nonlinear Control in the Year 2000*, volume 2 of *Lecture Notes in Control and Information Sciences*, pages 365–377. Springer-Verlag, 2001.

[4] P. A. Vela. *Averaging and control of nonlinear systems (with application to biomimetic locomotion)*. PhD thesis, California Institute of Technology, Pasadena, CA, May 2003.

[5] A. A. Agrachev and R. V. Gamkrelidze. The exponential representation of flows and the chronological calculus. *Matematicheskii Sbornik*, 149(4):467–532, 1978.

[6] K. Yagasaki and T. Ichikawa. Higher-order averaging for periodically forced weakly nonlinear systems. *International Journal of Bifurcation and Chaos*, 9(03):519–531, 1999.

[7] Hartono and A. H. P. Van Der Burgh. Higher-order averaging: periodic solutions, linear systems and an application. *Nonlinear Analysis: Theory, Methods & Applications*, 52(7):1727–1744, 2003.

[8] A. H. Nayfeh. *Perturbation Methods*. John Wiley and Sons, Inc., 1973.

[9] J. A. Sanders, F. Verhulst, and J. A. Murdock. *Averaging methods in nonlinear dynamical systems*, volume 2. Springer, 2007.

[10] F. Bullo. Averaging and vibrational control of mechanical systems. *SIAM Journal on Control and Optimization*, 41(2):542–562, 2002.

[11] G. K. Taylor and A. L. R. Thomas. Animal flight dynamics ii. longitudinal stability in flapping flight. *Journal of Theoretical Biology*, 214, 2002.

[12] G. K. Taylor and A. L. R. Thomas. Dynamic flight stability in the desert locust. *Journal of Theoretical Biology*, 206(6):2803–2829, 2003.

[13] G. K. Taylor and R. Zbikowski. Nonlinear time periodic models of the longitudinal flight dynamics of desert locusts. *Journal of Royal Society Interface*, 1(3):197–221, 2005.

[14] M. Sun and Y. Xiong. Dynamic flight stability of a hovering bumblebee. *Journal of Experimental Biology*, 208(3):447–459, 2005.

[15] M. Sun, J. Wang, and Y. Xiong. Dynamic flight stability of hovering insects. *Acta Mechanica Sinica*, 23(3):231–246, 2007.

[16] Y. Xiong and M. Sun. Dynamic flight stability of a bumble bee in forward flight. *Acta Mechanica Sinica*, 24(3):25–36, 2008.

[17] M. Richter and M. Patil. Influence of wing flexibility on the stability of flapping flight. In *AIAA Atmospheric Flight Mechanics Conference*, pages 2–5, 2010.

[18] J. M. Dietl and E. Garcia. Stability in ornithopter longitudinal flight dynamics. *Journal of Guidance, Control and Dynamics*, 31(4):1157–1162, 2008.

[19] N. Gao, H. Aono, and H. Liu. A numerical analysis of dynamic flight stability of hawkmoth hovering. *Journal of Biomechanical Science and Engineering*, 4(1):105–116, 2009.

[20] W. Su and C. E. S. Cesnik. Flight dynamic stability of a flapping wing micro air vehicle in hover. AIAA-Paper 2011-2009.

[21] I. Faruque and J. S. Humbert. Dipteran insect flight dynamics. part 1 longitudinal motion about hover. *Journal of theoretical biology*, 264(2):538–552, 2010.

[22] B. Cheng and X. Deng. Translational and rotational damping of flapping flight and its dynamics and stability at hovering. *IEEE Transactions On Robotics*, 27(5):849–864, 2011.

[23] H. Taha, S. Tahmasian, C. A. Woolsey, A. H. Nayfeh, and M. R. Hajj. The need for higher-order averaging in the stability analysis of hovering mavs/insects. 10(1):016002. Selected in the Bioinspiration & Biomimetics Highlights of 2015.

[24] H. Taha, A. H. Nayfeh, and M. R. Hajj. Effect of the aerodynamic-induced parametric excitation on the longitudinal stability of hovering mavs/insects. *Nonlinear Dynamics*, 78(4):2399–2408, 2014.

[25] H. Taha, C. A. Woolsey, and M. R. Hajj. Geometric control approach to longitudinal stability of flapping flight. *Journal of Guidance Control and Dynamics*, 39(2):214–226, 2016.

[26] A. Hassan and H. Taha. Differential-geometric-control formulation for flapping flight multi-body dynamics. *Submitted to Journal of Nonlinear Sciences*.

[27] R. C. Nelson. *Flight stability and automatic control*, volume 2. WCB/McGraw Hill New York, 1998.

[28] H. Taha, M. R. Hajj, and A. H. Nayfeh. On the longitudinal flight dynamics of hovering mavs/insects. *Journal of Guidance Control and Dynamics*, 37(3):970–978, 2014.

[29] A. L. R. Thomas and G. K. Taylor. Animal flight dynamics i. stability in gliding flight. *Journal of Theoretical Biology*, 212(1):399–424, 2001.

[30] L. Schenato, D. Campolo, and S. S. Sastry. Controllability issues in flapping flight for biomemetic mavs. volume 6, pages 6441–6447. 42nd IEEE conference on Decision and Control, 2003.

[31] X. Deng, L. Schenato, W. C. Wu, and S. S. Sastry. Flapping flight for biomemetic robotic insects: Part i system modeling. *IEEE Transactions on Robotics*, 22(4):776–788, 2006.

[32] X. Deng, L. Schenato, W. C. Wu, and S. S. Sastry. Flapping flight for biomemetic robotic insects: Part ii flight control design. *IEEE Transactions on Robotics*, 22(4):789–803, 2006.

[33] Z. A. Khan and S. K. Agrawal. Force and moment characterization of flapping wings for micro air vehicle application. pages 1515–1520. IEEE American Control Conference, 2005.

[34] Z. A. Khan and S. K. Agrawal. Control of longitudinal flight dynamics of a flapping wing micro air vehicle using time averaged model and differential flatness based controller. pages 5284–5289. IEEE American Control Conference, 2007.

[35] D. B. Doman, M. W. Oppenheimer, and D. O. Sigthorsson. Dynamics and control of a minimally actuated biomimetic vehicle, part i-aerodynamic model. Number 2009-6160, Chicago, Illinois. AIAA Guidance, Navigation, and Control Conference.

[36] M. W. Oppenheimer, D. B. Doman, and D. O. Sigthorsson. Dynamics and control of a minimally actuated biomimetic vehicle, part ii-control. Number 2009-6161, Chicago, Illinois. AIAA Guidance, Navigation, and Control Conference.

[37] D. B. Doman, M. W. Oppenheimer, and D. O. Sigthorsson. Wingbeat shape modulation for flapping-wing micro-air-vehicle control during hover. *Journal of Guidance, Control and Dynamics*, 33(3):724–739, 2010.

[38] M. W. Oppenheimer, D. B. Doman, and D. O. Sigthorsson. Dynamics and control of a biomimetic vehicle using biased wingbeat forcing functions: Part i: Aerodynamic model. Number 2010-1023. AIAA.

[39] D. B. Doman, M. W. Oppenheimer, and D. O. Sigthorsson. Dynamics and control of a biomimetic vehicle using biased wingbeat forcing functions: Part ii: Controller. AIAA-paper 2010-1024, Jan 2010.

[40] M. W. Oppenheimer, D. B. Doman, and D. O. Sigthorsson. Dynamics and control of a biomimetic vehicle using biased wingbeat forcing functions. *Journal Guidance, Control and Dynamics*, 34(1):204–217, 2011.

[41] H. Taha, A. H. Nayfeh, and M. R. Hajj. Aerodynamic-dynamic interaction and longitudinal stability of hovering mavs/insects. AIAA-Paper 2013-1707.

[42] H. Taha, M. R. Hajj, and P. S. Beran. Unsteady nonlinear aerodynamics of hovering mavs/insects. AIAA-Paper 2013-0504.

[43] H. Taha, M. R. Hajj, and P. S. Beran. State space representation of the unsteady aerodynamics of flapping flight. *Aerospace Science and Technology*, 34:1–11, 2014.

[44] G. J. Berman and Z. J. Wang. Energy-minimizing kinematics in hovering insect flight. *Journal of Fluid Mechanics*, 582(1):153,168, 2007.

[45] Hassan K Khalil. *Noninear Systems*. Prentice-Hall, New Jersey, 2002.

[46] C. P. Ellington. The aerodynamics of hovering insect flight: Ii. morphological parameters. *Philosophical Transactions Royal Society London Series B*, 305:17–40, 1984.

[47] C. T. Orlowski and A. R. Girard. Modeling and simulation of the nonlinear dynamics of flapping wing mavs. *AIAA Journal*, 49(5):969–981, 2011.

[48] C. T. Orlowski and A. R. Girard. Averaging of the nonlinear dynamics of flapping wing mav for symmetrical flapping. Aerospace Sciences Meeting, 2011.

[49] A. Banazadeh and N. Taymourtash. Adaptive attitude and position control of an insect-like flapping wing air vehicle. *Nonlinear Dynamics*, pages 1–20, 2016.

[50] Stabilization of an inverted pendulum under high-frequency excitation (kapitza pendulum). `https://www.youtube.com/watch?v=is_ejYsvAjY`.

[51] A. Stephenson. On an induced stability. *The London, Edinburgh, and Dublin Philosophical Magazine and Journal of Science*, 15(86):233–236, 1908.

[52] J. M. Berg and I.P. M. Wickramasinghe. Vibrational control without averaging. *Automatica*, 58:72–81, 2015.